

Small polarons and c -axis transport in highly anisotropic metals

A. F. Ho^{*1} and A. J. Schofield[†]

^{*} *The Abdus Salam ICTP, Strada Costiera 11, 34100 Trieste, Italy.*

[†] *School of Physics and Astronomy, Birmingham University, Edgbaston, Birmingham B15 2TT, U.K.*

Motivated by the anomalous c -axis transport properties of the quasi two-dimensional metal, Sr_2RuO_4 , and related compounds, we have studied the interlayer hopping of single electrons that are coupled strongly to c -axis bosons. We find a c -axis resistivity that reflects the in-plane electronic scattering in the low and very high temperature limits (relative to the characteristic temperature of the boson T_{boson}). For temperatures near the T_{boson} , a broad maximum in the resistivity can appear for sufficiently strong electron-boson coupling. This feature may account for the observed “metallic to non-metallic crossover” seen in these layered oxides, where the boson may be a phonon.

I. INTRODUCTION

Since the discovery of the cuprates, many studies have focused on the putative two dimensional (2d) non Fermi liquid state of the copper oxide layer in the normal state of these materials.² However, the superconducting state is three dimensional and, at least near to the superconducting critical temperature (T_c), some aspects of the physics of coupling between the planes must become important.³

The transport properties in the weakly-coupled dimension (denoted the c -axis here) are also interesting in their own right⁴. In the normal state of many of these layered copper oxides, the resistivity ratio, ρ_{ab}/ρ_c , is of order 10^3 to 10^5 but intriguingly, this ratio is temperature dependent: ρ_c is non-metallic near T_c , $\rho_c \sim T^{-\gamma}$, $0 < \gamma < 2$, while the in-plane resistivity has the marginal Fermi liquid behavior $\rho_{ab} \sim T$ (at least at optimal doping)⁴.

This dichotomous behavior cannot easily be accommodated within an anisotropic three dimensional (3d) Fermi surface picture. We begin with the assumption that the c -axis coupling is simply interlayer hopping of single electron:

$$H_c = t_c \sum_n c_{n+1}^\dagger c_n + h.c. , \quad (1)$$

where n is the layer index. Then, at temperatures larger than the c -axis electron hopping matrix element t_c , simple perturbation theory (to lowest order in t_c) with the Kubo formula gives the c -axis conductivity to be proportional to the polarization bubble (Fig. 1). In the figure, the thick lines represent the renormalised in-plane Green's function. Hence the c -axis conductivity directly reflects the *in-plane* spectral weight. But if the in-plane state is a metal, then the c -axis conductivity should also be metallic.

There are at least two ways to bypass this argument. Either the in-plane physics is unusual or the interlayer coupling is unconventional. Considering the first possibility, there might be a non Fermi liquid in-plane Green's function⁵. More conventionally, Ioffe and Millis⁶ argued for superconducting phase fluctuations, and others have just assumed some phenomenological form of in-plane spectral weight which has strong in-plane scat-

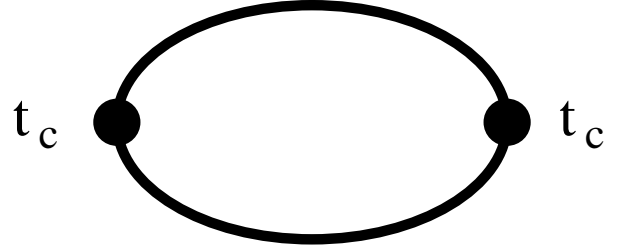


FIG. 1: The order t_c^2 contribution to the c -axis conductivity. The thick lines represent the renormalised in-plane Green's function.

tering built-in⁷. In such schemes, the interlayer transport directly probes the anomalous in-plane scattering. Within the second possibility, Rojo and Levin⁸ considered static disorder, and also boson-assisted hopping in the c -axis direction, while Turlakov and Leggett⁹ studied interplane and in-plane charge fluctuations. These approaches can lead to incoherent c -axis transport, without the need to invoke strongly anomalous in-plane behavior.

Motivated by experiments in a related system, the strontium ruthenate family, we follow the second route in this paper and study a boson-assisted hopping mechanism for the unusual c -axis transport in the ruthenate systems.

In contrast to previous work on boson-assisted hopping⁸, in this report we treat the strong c -axis electron-boson coupling *exactly* via a canonical transformation, and then add the weak c -axis hopping perturbatively. Thus the essential physics is that of the small polaron.^{10,11} This can be seen most easily after the canonical transformation: when the electron hops from one plane $n + 1$ to another at n , a cloud of bosons are created or destroyed:

$$c_n^\dagger c_{n+1} \xrightarrow[\text{transf.}]{\text{canon.}} c_n^\dagger c_{n+1} \exp \left[\sum_q A_n(q) (a_q - a_{-q}^\dagger) \right], \quad (2)$$

(The precise form of the amplitude $A_n(q)$ is shown in Eq. 7 below.) At temperatures lower than the characteristic energy of the boson, T_{boson} , electrons can hop from

one plane to another, but this hopping is suppressed due to the “dragging” of the boson cloud. With increasing T , more and more bosons are created and destroyed; due to this inelastic scattering process, the hopping electron acquires a large imaginary part in the self-energy: interlayer hopping becomes more like diffusive. Hence a crossover into a non-metallic behaviour occurs.

Note that there is a crucial separation of scales. We assume that, because of the highly anisotropic electronic dispersion in these quasi-2d materials, $\epsilon_{\text{Fermi}}^{\text{in-plane}} \gg T_{\text{boson}} \gg t_c$. Thus, it is possible for the strong electron-boson coupling to show up dramatically in c -axis transport, while the in-plane behavior is relatively unaffected. Also, it allows us to treat the c -axis hopping perturbatively and still have quantitative control over the crossover region near T_{boson} .

In this paper, we shall concentrate on the d.c. resistivity in the c -direction. Our main finding is, indeed, that due to the small polaron, a metal to non-metal crossover for temperatures near the boson scale T_{boson} is obtained. At higher or lower temperatures, the c -axis transport basically reflects the in-plane dynamics through the in-plane scattering rate.

We have so far not specified the nature of the boson. This is because the analysis to be presented can, in general, be applied to any kind of strong electron-boson coupling, provided there is this separation of scales mentioned, and the bosonic mode is gapped and neutral. For the rest of the paper, we shall phrase the analysis in terms of phonons, with a view towards application to some members of the strontium ruthenate family. For other members of the same family with known magnetic instabilities, and perhaps for the cuprates, this boson could be a paramagnon or other magnetic excitation.

Strontium ruthenate Sr_2RuO_4 is iso-structural to one of the parent compounds of the cuprates, La_2CuO_4 . Above its superconducting transition temperature of 1.5K , it is a well-characterised 3d Fermi liquid¹², and yet, above a coherence scale of $\sim 25\text{K}$, the c -axis optical conductivity loses its Drude peak¹³, and above a “crossover” scale, $T_{\text{max}} \sim 130\text{K}$, the c -axis resistivity becomes non-metallic while the ab -plane resistivity stays metallic, albeit with a close to linear temperature dependence and a value which eventually exceeds the Mott-Ioffe-Regel limit¹⁴. In the recent report of Jin *et. al.*¹⁵ in the related system $\text{Ca}_{1.7}\text{Sr}_{0.3}\text{RuO}_4$, where there is the same dichotomous resistivity behaviour, $T_{\text{max}} \sim 190\text{K}$ appears to be tied to a structural phase transition. In Sr_2RuO_4 , there is no such direct link, but there are strong electron-phonon interactions in the c -direction.¹⁶ This motivates us to consider phonon-assisted hopping as a potential origin for the non-metallic ρ_c in these systems at high temperatures.

A further experimental observation in the vicinity of T_{max} in the c -axis resistivity is that the magnetoresistance can change sign and becomes negative above T_{max} . This happens¹⁹ in both the longitudinal (field parallel to the current) and transverse (field perpendicular to the

current) directions in Sr_2RuO_4 . Somewhat similar properties can be found in some of the cuprates, although there seems to be no universality in the c -axis magnetoresistance between the various families of the cuprates.²⁰ In this paper, we shall calculate the orbital component of the magnetoresistance. This will necessarily be positive and will not explain these observations. However, a more complete theory would need to take into account the effect of magnetic field on the propagators and the bosonic mode, which is beyond the scope of this paper, but we will argue that it must be these contributions that change the sign of the magnetoresistance, within this picture at least.

The plan of the paper is as follows: in Section II, we define our model, in Section III, we study the model in the strong electron-phonon coupling limit. Section IV gives the results. Section V discusses the relevance of this model to the strontium ruthenate family and beyond.

II. MODEL

As already emphasized in the Introduction, the analysis to be presented can be applied generally, with little modification, to any strong coupling of electrons to a gapped, neutral bosonic mode, but to be concrete, we shall consider coupling to phonons.

Our model involves electrons coupled to the polarisation induced by the out of phase vibration of the ions within a unit cell; the form of this electron-optical phonon coupling has been derived long ago in the 3d case²¹:

$$H_{\text{e-ph}}^{3d} = \sum_n \int d^2x \sum_{\vec{q}} M_{\vec{q}} \exp(i\vec{q}\vec{R}_n) \rho_n(\vec{x}) (a_{\vec{q}} + a_{-\vec{q}}^\dagger), \quad (3)$$

where $\vec{R}_n = [\vec{x}, z_n]^T$, \vec{x} is the intraplane coordinate, $z_n = nc$ is the plane coordinate, with c the interlayer distance and n the plane index. $\rho_n(\vec{x}) = c_n^\dagger(\vec{x})c_n(\vec{x})$ is the electronic density. The electrons mainly couple to longitudinal phonons (represented by $a_{\vec{q}}, a_{\vec{q}}^\dagger$) because only these phonons set up strong enough electric fields when they vibrate²³. Then the direction of the polarisation vector locally is simply along the direction given by the vector sum of the displacements of the ions in a unit cell. Now, for the mode that can couple to c -axis charge transport, we expect that in these highly anisotropic metals such as the cuprates and Sr_2RuO_4 , the effective force constant between the planes may be less stiff than those within the plane. This is because of the strong covalent bonding and the strong band electronic correlation within the plane, as compared to the weaker bonding and correlations between the planes. Effectively, due to the large in-plane effective force constants, we let the vibration frequency for the in-plane modes $\omega_{\vec{q}} \rightarrow \infty$ compared to the interplanar one. In any case, we wish to separate out the direct effect of strong electron-phonon coupling on c -axis transport, from the effect of phonons

on in-plane propagation which then influences the c -axis transport via the mechanism sketched in Fig. 1. Thus, with such a simplification, the Fourier transform of the displacement vector \vec{Q} is only in the interplane direction: $\vec{Q} \propto \vec{q}(\omega_{\vec{q}})^{-1/2}(a_{\vec{q}} + a_{-\vec{q}}^\dagger) \approx [0, 0, Q_c]^T$, with $Q_c \propto (\omega_{\vec{q}})^{-1/2}(a_{\vec{q}} + a_{-\vec{q}}^\dagger)$, and the propagation direction q (not a vector!) is along the c -axis. In effect, all the ions in a plane oscillate together rigidly, in the direction perpendicular to the plane, and the propagation direction is also parallel to the c -axis. Hence it is the total charge $\rho_n = \int d^2x c_n^\dagger(\vec{x})c_n(\vec{x})$ of the n 'th plane that couples to the phonon creation and annihilation operators a_q^\dagger, a_q :

$$H_{\text{e-ph}} = \sum_n \sum_q M_q \exp(iqz_n) \rho_n (a_q + a_{-q}^\dagger), \quad (4)$$

where we have combined all the prefactors as usual into the electron-phonon coupling M_q .

If the bosonic mode is of magnetic origin, we may argue that because of stronger electronic overlaps in-plane compared to the interplane direction, and hence stronger in-plane exchange effects, the magnetic fluctuation mode is softer in the interplane direction, and again this simplified form of electron-boson coupling will be appropriate.

Our model Hamiltonian is thus:

$$\begin{aligned} H &= \sum_n H^{(n)} + H_c + H_{\text{e-ph}} + H_{\text{ph}}, \\ H_c &= \int d^2x \sum_n t_c c_{n+1}^\dagger(\vec{x})c_n(\vec{x}) + \text{H.c.} \quad , \\ H_{\text{e-ph}} &= \sum_n \sum_q M_q \exp(iqz_n) \rho_n (a_q + a_{-q}^\dagger), \\ H_{\text{ph}} &= \sum_q \omega_q a_q^\dagger a_q. \end{aligned} \quad (5)$$

The model system consists of a stack of $2d$ planes described by $H^{(n)}$. We shall take this as a phenomenological input, characterised by a $2d$ Green's function or equivalently, a $2d$ spectral weight.

In H_c , electrons are assumed to hop from one plane directly to a neighbouring plane only, at the same \vec{x} ; in momentum space, this means that the c -axis hopping matrix element t_c is independent of the in-plane momentum. (This ignores the complication of staggered planes in the cubic perovskite structure and the multiband nature of Sr_2RuO_4 , see Discussion.) For simplicity, we have left out the spin index on the electron operators $c_n(\vec{x})$.

$H_{\text{e-ph}}$ describes the electron-optical phonon interaction in the c -direction, as detailed above. We have left the electron-phonon coupling M_q unspecified: as we shall see, it enters only within an electron-phonon parameter $[\Delta$ or $\gamma(T)$ depending on the phonon dispersion, see Methods].

For H_{ph} , The c -axis optical phonons have a dispersion ω_q ; in this paper we shall look closely at the Einstein phonon $\omega_q \sim \omega_0$. This is both because optical phonons tend to have little dispersion relative to the acoustic ones,

and also we are able to obtain many explicit analytical results. We shall also discuss somewhat more qualitatively the opposite case of a generic dispersion where the phonon density of state does not have any sharp features. These two forms of dispersion can be thought of as opposite limits: the Einstein phonon is the limit where all phonon modes (of different wavevector q) have the same energy, while the more general dispersion corresponds to the limit when all phonon modes are non-degenerate.

III. METHODS

A. Canonical Transformation

The key physics we are looking for is the effect of strong electron-phonon coupling on the charge transport in the weakest direction, the c -axis. Physically, the motion of the electron is accompanied by the emission and absorption of a large number of phonons due to the strong coupling, forming the so-called small polaron¹⁰. Technically, one must deal with the large term $H_{\text{e-ph}}$ first, and add the inter-plane tunneling H_c later as a perturbation. The former is accomplished by the canonical transformation, $\bar{H} = \exp(-S)H\exp(S)$, a straightforward generalisation of the transformation well-known in the small polaron problem^{22,23}:

$$\begin{aligned} S &= \int d^2x S(\vec{x}), \\ S(\vec{x}) &= - \sum_{n,q} \frac{M_q}{\omega_q} e^{iqR_n} c_n^\dagger(\vec{x})c_n(\vec{x}) (a_q - a_{-q}^\dagger). \end{aligned} \quad (6)$$

One finds then,

$$\begin{aligned} \bar{H} &= \sum_n H^{(n)} + \int d^2x \bar{H}_c(\vec{x}) + H_{\text{ph}}, \\ \bar{H}_c(\vec{x}) &= - \sum_{n,q} \frac{|M_q|^2}{\omega_q} c_n^\dagger(\vec{x})c_n(\vec{x}) \\ &\quad + \sum_n t_c c_{n+1}^\dagger(\vec{x})c_n(\vec{x}) X_{n+1}^\dagger X_n + \text{H.c.} \quad , \\ X_n &= \exp \left\{ \sum_q \frac{M_q}{\omega_q} e^{iqR_n} (a_q - a_{-q}^\dagger) \right\}. \end{aligned} \quad (7)$$

Thus strong electron-phonon coupling leads to, (1) a renormalisation of the in-plane chemical potential (first term of \bar{H}_c), which we shall henceforth ignore, and (2) an effective vertex correction for the c -axis hopping t_c (second term of \bar{H}_c). Note that since the phonon modes couple to the *total* charge density in a plane, $\bar{H}^{(n)} = \exp(-S)H^{(n)}\exp(S) = H^{(n)}$: the in-plane motion of the electron is not in the presence of the interplane polaronic effects, within this simplified model.

B. Linear Response: conductivity and magneto-conductivity

In this paper, we look at the zero-frequency conductivity and the magnetoconductivity. For the conductivity, since the charge in the n 'th plane is $Q_n^c = e \int d^2x c_n^\dagger(\vec{x})c_n(\vec{x})$, the current in the c -direction is just $j_n^c = \partial_t Q_n^c = -i[Q_n^c, H]$. After the canonical transformation, $\bar{j}_n^c = -i[Q_n^c, \bar{H}_c]$, and so:

$$\langle \bar{j}_n^c \rangle = iet_c \int d^2x \left\langle \left[c_{n+1}^\dagger(\vec{x})c_n(\vec{x})X_{n+1}^\dagger X_n - \text{h.c.} \right] \right\rangle. \quad (8)$$

Using the Kubo formula and expanding to $O(t_c^2)$ gives the conductivity, ie., the linear response to an applied electric field in the c -direction $\sigma_c = \bar{j}^c/E_c$:

$$\begin{aligned} \sigma_c(k_c = 0, \Omega = 0) &= \lim_{\Omega \rightarrow 0} \frac{e^2 t_c^2}{\Omega} \sum_n \int d^2k_{\parallel} \int d\tau \\ &\times e^{i\Omega\tau} U(\tau) G_n^{(2d)}(\vec{k}_{\parallel}, \tau) G_{n+1}^{(2d)}(\vec{k}_{\parallel}, \tau), \\ U(\tau) &= \left\langle X_{n+1}^\dagger(\tau) X_n(\tau) X_n^\dagger(0) X_{n+1}(0) \right\rangle_{H_{\text{ph}}}. \end{aligned} \quad (9)$$

where $G_n^{(2d)}(\vec{k}_{\parallel})$ is the in-plane (dressed) Green's function for the plane n at in-plane momentum \vec{k}_{\parallel} . In Fourier space, the effect of strong electron-phonon coupling is to induce an effective ω -dependent vertex $t_c^2 \rightarrow t_c^2 U(\omega)$. Classically, the phonon correlation function $U(\omega)$ leads to a Debye-Waller factor.

For magnetoresistance, we shall only study the case where the magnetic field lies in-plane, avoiding the complication of magnetic field induced orbital effects on the in-plane propagators. We also do not consider spin effects here, see Discussion. As \vec{B} does not couple directly to the phonons, its sole effect is on the orbital motion of the electrons, which can be dealt with by the usual Peierls substitution $\vec{p} \rightarrow \vec{p} - e\vec{A}$. With $\vec{B} = (B, 0, 0)$, the associated vector potential (in the Landau gauge) is $\vec{A} = (0, -zB, 0)$. Choose plane $n = 1$ to have c -axis coordinate $z = 0$, and for plane $n = 2$, $z = c$ where c is the interplane distance. Hence,

$$\begin{aligned} G_{n=1}^{(2d)}(\vec{k}_{\parallel}) &\rightarrow G_{n=1}^{(2d)}(\vec{k}_{\parallel}), \\ G_{n=2}^{(2d)}(\vec{k}_{\parallel}) &\rightarrow G_{n=2}^{(2d)}(\vec{k}_{\parallel} + \vec{q}_B), \\ \vec{q}_B &= e\vec{c} \times \vec{B}, \end{aligned} \quad (10)$$

where \vec{c} is a vector of length c pointing in the positive c -direction, and \vec{k}_{\parallel} is the in-plane momentum.

To massage the (magneto) conductivity into a more familiar form, we introduce the usual spectral representations:

$$\begin{aligned} G_n^{(2d)}(\vec{k}_{\parallel}, \omega_m) &= \int dz \frac{A^{(2d)}(\vec{k}_{\parallel}, z)}{i\omega_m - z}, \\ U(\nu_n) &= \int dz \frac{B(z)}{i\nu_n - z}. \end{aligned}$$

where $\omega_m = (2m+1)\pi T$ is an odd Matsubara frequency, and $\nu_n = 2n\pi T$ is an even Matsubara frequency. T is the temperature. Note that since there is translation invariance in the c -direction, we have dropped the plane index n in the spectral functions $A^{(2d)}(\vec{k}_{\parallel}, z)$ and $B(z)$. Fourier transforming with respect to the imaginary time in Eq. (9), and doing the Matsubara sums leads to the d.c. conductivity:

$$\begin{aligned} \sigma_c(T, \vec{q}_B) &= \frac{e^2 N_c t_c^2}{T} \int d\omega d\nu \int \frac{d^2k_{\parallel}}{(2\pi)^2} \\ &\times A^{(2d)}(\vec{k}_{\parallel} + \vec{q}_B, \omega + \nu) A^{(2d)}(\vec{k}_{\parallel}, \nu) \\ &\times \left[\frac{f(\nu) - f(\omega + \nu)}{\omega} \right] D(\omega, T), \\ D(\omega, T) &= \omega B(\omega) n^B(\omega) [1 + n^B(\omega)]. \end{aligned} \quad (12)$$

where N_c is the number of planes in the c -direction, $f(\nu) = 1/(\exp[\nu/T] + 1)$ is the Fermi function, and $n^B(\omega) = 1/(\exp[\omega/T] - 1)$ is the Bose function. $D(\omega, T)$ is essentially the phonon spectral weight multiplied by the Bose factors.

C. Phonon Spectral Function

To get the phonon spectral function $B(\omega)$, we need:

$$B(\omega) = -\frac{1}{\pi} \text{Im} U^{\text{ret}}(\omega) = -\frac{1}{\pi} \text{Im} \int_{-\infty}^{+\infty} e^{i\omega t} U^{\text{ret}}(t), \quad (13)$$

where the retarded real time spectral function is just:

$$U^{\text{ret}}(t) = -i\theta(t) \left\langle \left[X_{n+1}^\dagger(t) X_n(t), X_n^\dagger(0) X_{n+1}(0) \right] \right\rangle_{H_{\text{ph}}} \quad (14)$$

with $X_n(t)$ given in Eq. 7.

The calculation of $U^{\text{ret}}(t)$ proceeds along the same line as in the small polaron model (see Mahan²³, Ch. 6.2), and we get the exact result:

$$\begin{aligned} U^{\text{ret}}(t) &= -i\theta(t) 2e^{\sum_q F_q [n^B(\omega_q)(1+n^B(\omega_q)) - (2n^B(\omega_q)+1)]} \\ &\times \{ \cos[\omega_q(t + i/2T)] - \cos[\omega_q(-t + i/2T)] \} \end{aligned} \quad (15)$$

where $F_q = \left| \frac{M_q}{\omega_q} \right|^2 2(1 - \cos q) > 0$, and $n^B(\omega_q) = 1/(\exp(\omega_q/T) - 1)$.

In this paper, we look at two types of phonon dispersion: (1) Einstein phonon where $\omega_q = \omega_0$ for all q , and (2) a generic dispersion such that there are no sharp features in the phonon density of state. Again, the calculation is directly analogous to that of the small polaron problem, see e.g. chapter 4 of Ref.²³ for details of the calculation.

For the Einstein phonon, setting $\omega_q = \omega_0$ in Eq. 15, putting this form into Eq. 13, and using the Bessel function identity $\exp(z \cos(\phi)) = \sum_{n=-\infty}^{+\infty} I_n(z) \exp(in\phi)$, the spectral function can be expressed as an infinite sum of

Bessel functions of the imaginary kind:

$$B(\omega) = 2e^{-2S_T} \times \sum_{n=-\infty}^{+\infty} I_n(\Lambda(T)) \sinh\left(\frac{n\omega_0}{2T}\right) \delta(\omega - n\omega_0), \quad (16)$$

where

$$\begin{aligned} \Lambda(T) &= (\Delta/\omega_0)^2 / \sinh(\omega_0/2T), \\ \Delta^2 &= \sum_q |M_q|^2 2(1 - \cos q), \\ 2S_T &= (\Delta/\omega_0)^2 \coth(\omega_0/2T). \end{aligned} \quad (17)$$

Thus the function $D(\omega, T)$ defined in Eq. 12 becomes:

$$D(\omega, T) = e^{-2S_T} \left\{ T I_0(\Lambda) \delta(\omega) + \frac{\omega}{2 \sinh(\omega/2T)} \sum_{n=1}^{\infty} I_n(\Lambda) [\delta(\omega - n\omega_0) + \delta(\omega + n\omega_0)] \right\}. \quad (18)$$

For the more general dispersion, the time integral has to be approximated. As in the small polaron problem, one appeals to the fact that this is at strong electron-phonon coupling, and so the dimensionless factor F_q in the exponential in Eq. 15 is large, and the integral can be done using the saddle point approximation:

$$B(\omega) \simeq \frac{1}{\sqrt{\pi\gamma^2}} \sinh(\omega/2T) e^{-\omega^2/4\gamma^2} \times \exp \left\{ - \sum_q F_q \left[\sqrt{n^B(\omega_q) + 1} - \sqrt{n^B(\omega_q)} \right]^2 \right\}, \quad (19)$$

with $\gamma^2 = \sum_q |M_q|^2 (1 - \cos q) / \sinh(\omega_q/2T)$ and F_q is as before (see after Eq. 15). And the function $D(\omega, T)$ becomes:

$$D(\omega, T) \simeq \frac{1}{4\sqrt{\pi\gamma^2}} \frac{\omega}{\sinh(\omega/2T)} e^{-\omega^2/4\gamma^2} \times \exp \left\{ - \sum_q F_q \left[\sqrt{n^B(\omega_q) + 1} - \sqrt{n^B(\omega_q)} \right]^2 \right\}. \quad (20)$$

D. Calculation of σ_c

It is advantageous to do the in-plane momentum integrals first. Note that the ratio of the magnetic wavevector $\vec{q}_B = e\vec{c} \times \vec{B}$ (Eq. 11) to the in-plane Fermi momentum k_F is:

$$\frac{q_B}{k_F} \sim \frac{ecB}{\pi/2a} = \frac{2acB}{\Phi_0} \quad (21)$$

where $\Phi_0 = h/2e$ is the unit flux quantum, a is the in-plane lattice spacing, c is the interlayer distance. For

Sr_2RuO_4 , $a = 3.87\text{\AA}$ $c = 6.37\text{\AA}$ around room temperature, and so,

$$\frac{q_B}{k_F} \sim 3 \cdot 10^{-4} \cdot B \quad (B \text{ in tesla}). \quad (22)$$

Thus for the in-plane electronic dispersion, we can approximate $\epsilon_{\vec{k}+\vec{q}_B} \simeq \epsilon_{\vec{k}} + \vec{v} \cdot \vec{q}_B$ with $\vec{v} = \partial\epsilon_{\vec{k}}/\partial\vec{k}$.

We simplify further with the choice of a flat band of width $2D$ and a circular (in-plane) Fermi surface. Then $\int d^2k \rightarrow N_0 \int_{-D}^D d\epsilon \int_0^{2\pi} \frac{d\theta}{2\pi}$, where N_0 is the 2d density of state at the Fermi surface. For the isotropic in-plane Fermi surface, we pick \vec{q}_B to lie in the direction of \hat{k}_x , and thus, $\epsilon_{\vec{k}+\vec{q}_B} \simeq \epsilon_{\vec{k}} + v_F q_B \cos(\theta)$. For simplicity, we have taken \vec{B} to lie entirely in the plane, hence $q_B = ecB$.

Write the 2d spectral weight in the form:

$$A^{(2d)}(\vec{k}, \omega) = \frac{1}{\pi} \frac{\Gamma(\omega)}{(\omega - \epsilon_{\vec{k}})^2 + \Gamma(\omega)^2}, \quad (23)$$

where we assume that the scattering rate $\Gamma(\omega)$ has little in-plane momentum dependence. As all energy scales will be small compared to the bandwidth $2D$, we can set $D \rightarrow \infty$, and we find then,

$$\begin{aligned} &\int d^2k A^{(2d)}(\vec{k} + \vec{q}_B, \omega + \nu) A^{(2d)}(\vec{k}, \omega) \\ &\simeq \frac{N_0}{\pi} \text{Re} [(v_F q_B)^2 - (\nu + i\Gamma_{\text{tot}}(T, \omega, \nu))^2]^{-1/2}, \end{aligned} \quad (24)$$

where $\Gamma_{\text{tot}}(T, \omega, \nu) = \Gamma(T, \omega) + \Gamma(T, \omega + \nu)$.

Substituting Eq. 24 into Eq. 12 leads finally to the zero-frequency, zero-momentum c -axis conductivity:

$$\begin{aligned} \sigma_c(T, B) &= \frac{e^2 N_0 N_c t_c^2}{\pi T} \text{Re} \int d\omega d\nu \frac{f(\omega) - f(\omega + \nu)}{\nu} \\ &\times \frac{D(\nu, T)}{[(v_F q_B)^2 - (\nu + i\Gamma_{\text{tot}}(T, \omega, \nu))^2]^{1/2}}. \end{aligned} \quad (25)$$

This is the key equation we shall analyse in the next section. It is worth summarizing the assumptions used in deriving this: (i) \vec{B} lies in-plane and is small, (ii) flat band, circular Fermi surface, (iii) in-plane spectral weight has a scattering rate that has little momentum dependence, and (iv) second order perturbation theory in t_c .

IV. RESULTS

A. Einstein phonons

Because of the totally degenerate spectrum $\omega_q = \omega_0$, the function $D(\omega, T)$ (Eq. 18) is made up of delta functions at the harmonics $\omega = n\omega_0$, $n = 0, \pm 1, \pm 2, \dots$. Putting this form into Eq. 25 for a general in-plane scattering $\Gamma(T, \omega)$, we get the exact result:

$$\sigma_c(T, B) = \frac{e^2 N_0 N_c t_c^2}{\pi} e^{-2S_T} \int d\nu \left\{ \frac{-\partial f}{\partial \nu} \frac{a_0(\Lambda(T))}{\sqrt{(v_F e c B)^2 + (\Gamma_{\text{tot}}(T, 0, \nu))^2}} \right. \\ \left. + \sum_{n=1}^{\infty} \left[a_n(\Lambda(T)) \frac{f(\nu) - f(\nu + n\omega_0)}{n\omega_0} \text{Re} \frac{1}{\sqrt{(v_F e c B)^2 + (\Gamma_{\text{tot}}(T, n\omega_0, \nu) - i n\omega_0)^2}} + (\omega_0 \rightarrow -\omega_0) \right] \right\}, \quad (26)$$

where $a_0(\Lambda) = I_0(\Lambda)$, $a_n(\Lambda) = I_n(\Lambda) \frac{n\omega_0/2T}{\sinh(n\omega_0/2T)}$, and $I_n(z)$ are the Bessel functions of imaginary kind. One can show that the amplitude, a_n , decreases with increasing n . In the experimentally accessible range of temperatures (at most a few times of $T_{\text{Debye}} \sim 500K$), one only needs the first few harmonics (n) in Eq. (26). This is because the higher harmonics contribute little to the low T and small B behaviour, thanks to both the amplitude $a_n(\Lambda)$ getting smaller and the denominator of Eq. 26 getting larger with higher n .

To determine the asymptotes, note that the various parameters of the Einstein phonon model have the limiting values (see after Eq. 16 for their definitions):

$$\Lambda(T) \rightarrow \begin{cases} \left(\frac{\Delta}{\omega_0}\right)^2 \frac{2T}{\omega_0} & : T \gg \omega_0, \\ \left(\frac{\Delta}{\omega_0}\right)^2 2e^{-\omega_0/2T} & : T \ll \omega_0, \end{cases} \quad (27)$$

$$2S_T \rightarrow \begin{cases} \left(\frac{\Delta}{\omega_0}\right)^2 \frac{2T}{\omega_0} & : T \gg \omega_0, \\ \left(\frac{\Delta}{\omega_0}\right)^2 & : T \ll \omega_0, \end{cases}$$

where $\Delta^2 = \sum_q |M_q|^2 2(1 - \cos q)$ characterises the strength of the electron-phonon interaction. The argument $\Lambda(T)$ of the Bessel function is always small in the low T limit, but it can be large or small in the high T limit, depending on the magnitude of Δ/ω_0 via the combination $(\Delta/\omega_0)^2 (T/\omega_0)$.

Substituting the asymptotic forms Eq. 27 into Eq. 26, and using the expansions for Bessel function, we get for low temperatures $T \ll \omega_0$, (or for high T with $(\Delta/\omega_0)^2 (T/\omega_0) \ll 1$):

$$\sigma_c \simeq \frac{e^2 N_0 N_c t_c^2}{\pi} \frac{e^{-(\Delta/\omega_0)^2}}{\sqrt{(v_F e c B)^2 + 4\Gamma(T, 0)^2}}. \quad (28)$$

We have dropped $n > 0$ terms, as they are of order $e^{-n\omega_0/T}$ relative to the $n = 0$ term. Also, both the marginal Fermi liquid and the Fermi liquid scattering rate varies relatively slowly compared to $\partial f/\partial \nu$, and hence we have approximated $-\partial f/\partial \nu \sim \delta(\nu)$ to get the above equation. Note that in this low T limit, the effective bandwidth t_c gets renormalised by the phonons by the factor $\exp[-(\Delta/\omega_0)^2/2]$.

For high temperatures $T \gg \omega_0$ and $\Delta/\omega_0 > 1$:

$$\sigma_c \simeq \frac{e^2 N_0 N_c t_c^2}{\pi} \frac{1 + O(\omega_0/T)}{\sqrt{2\pi \left(\frac{\Delta}{\omega_0}\right)^2 \frac{2T}{\omega_0}}} \quad (29)$$

$$\times \left\{ \frac{1}{\sqrt{(v_F e c B)^2 + 4\Gamma(T, 0)^2}} + 2\text{Re} \frac{1}{\sqrt{(v_F e c B)^2 + (2\Gamma(T, \omega_0) - i\omega_0)^2}} + (\text{higher harmonics}) \right\}.$$

Again, we have made the approximation $(f(\nu) - f(\nu + n\omega_0))/n\omega_0 \sim -\partial f/\partial \nu \sim \delta(\nu)$, the first approximation being valid as $T \gg \omega_0$, and the second approximation is due to the same reason as mentioned for the low temperature case. Notice that the leading terms in both the high- and low-temperature limits do not have any $e^{-\Delta/T}$ factors, in contrast to the general phonon dispersion case below.

The precise low and high T -dependence at $B = 0$ reflects the form of the in-plane scattering. For a marginal Fermi liquid form:

$$\Gamma(T, \omega) = \alpha_{\text{MFL}} \omega \coth(\omega/T), \quad (30)$$

the asymptotics from Eqns. 28, 29 are:

$$\sigma_c(T \ll \omega_0) \sim T^{-1} \quad (31)$$

$$\sigma_c(T \gg \omega_0) \sim T^{-3/2}$$

while for a Fermi liquid form:

$$\Gamma(T, \omega) = \alpha_{\text{FL}} \frac{\omega^2 + (\pi T)^2}{\epsilon_F}, \quad (32)$$

the asymptotics are:

$$\sigma_c(T \ll \omega_0) \sim T^{-2} \quad (33)$$

$$\sigma_c(T \gg \omega_0) \sim T^{-5/2}$$

The above asymptotics miss out the experimentally important and interesting regime of $T \approx \omega_0$. A broad maximum appears when T is somewhat below ω_0 , *only* when $\Delta/\omega_0 \gtrsim 2$. Also, the maximum grows rapidly with increasing Δ/ω_0 . This occurs because of two competing factors: see Eq. 26. For $\Delta/\omega_0 \gg 1$, $\Lambda(T)$ is again

large, and we can use the asymptotic form for the Bessel functions, while keeping $T \approx \omega_0$:

$$\sigma_c \propto \sqrt{\sinh(\omega_0/2T)} \exp\left(-\left[\frac{\Delta}{\omega_0}\right]^2 2 \frac{\sinh^2(\omega_0/4T)}{\sinh(\omega_0/2T)}\right) \times \left\{ \frac{1}{[(v_F e c B)^2 + (2\Gamma(T, 0))^2]^{1/2}} + \dots \right\}, \quad (34)$$

where we have dropped higher harmonics (which change the magnitude, but not the general T -dependence). Thus there are two opposing tendencies: the phonon contributed part (the exponential and the square root of \sinh) which grows with T , versus the in-plane scattering part $\Gamma(T, 0) \propto T$ for the marginal Fermi liquid. The result is the broad maximum structure in σ_c (Fig. 2,3). Note that the height of the maximum has a strong dependence on the strength of the electron-phonon coupling Δ . In a Fermi liquid the in-plane scattering rate $\sim T^2$ damps out the phonon contributed parts more strongly and to see this structure, one needs to go to larger Δ/ω_0 .

We have estimated the critical phonon parameter Δ_c/ω_0 and the position of the maximum T_{\max} and the concomitant minimum T_{\min} from Eq. 26 by taking into account only the zeroth harmonics $n = 0$. For an in-plane scattering rate of the form $\Gamma(T) = \alpha T^\eta$,

$$\frac{\Delta_c}{\omega_0} \approx \sqrt{\frac{\eta}{0.4}}, \quad (35)$$

and the broad maximum only appears when $\Delta > \Delta_c$. The critical temperature when the broad maximum starts to appear, *i.e.* when T_{\max} starts to be different from T_{\min} , occurs at:

$$T_{\text{crit}} \approx \omega_0/3.0. \quad (36)$$

For Δ only slightly larger than Δ_c , both T_{\max} and T_{\min} are close to T_{crit} :

$$\frac{\omega_0}{2T_{\max/\min}} \approx \frac{\omega_0}{2T_{\text{crit}}} \pm \sqrt{\frac{\eta}{0.2} \left[\left(\frac{\omega_0}{\Delta_c} \right)^2 - \left(\frac{\omega_0}{\Delta} \right)^2 \right]}. \quad (37)$$

For large Δ/ω_0 , T_{\max} and T_{\min} obey the approximate equations:

$$\begin{aligned} \frac{\Delta^2}{\omega_0^2} &\approx \frac{\eta T_{\max}}{\omega_0} \exp\left(\frac{\omega_0}{2T_{\max}}\right), \\ \frac{\Delta^2}{\omega_0^2} &\approx \frac{4\eta T_{\min}}{\omega_0}. \end{aligned} \quad (38)$$

Note that both T_{\max} and Δ_c depend mainly on phonon parameters; one can show that the in-plane scattering rate enters only in the form of the exponent η . In particular, both T_{\max} and T_{\min} can only depend on the scale ω_0 . Hence the width of the broad maximum, roughly given by $2(T_{\max} - T_{\min})$, is governed by the scale ω_0 .

Fig. 2 illustrates the resistivity (the inverse of the conductivity) of Eq. 26 for a range of values of Δ , using a marginal Fermi liquid form for the in-plane scattering, and including up to $n = 5$ harmonics of ω_0 . Fig. 3 shows the Fermi liquid case, where the maximum is much less prominent than in the marginal Fermi liquid case, as already mentioned.²⁴ All energies are measured in units of ω_0 . ρ_c is measured in units of $\pi/e^2 N_0 N_c t_c^2$.

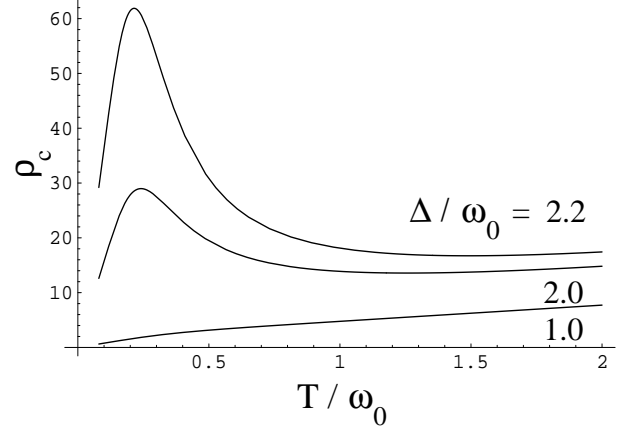


FIG. 2: $B = 0$ c -axis resistivity with in-plane marginal Fermi liquid scattering (Eq. 30) for electrons coupled to c -axis Einstein phonons, $\alpha_{\text{MFL}} = 1.0$

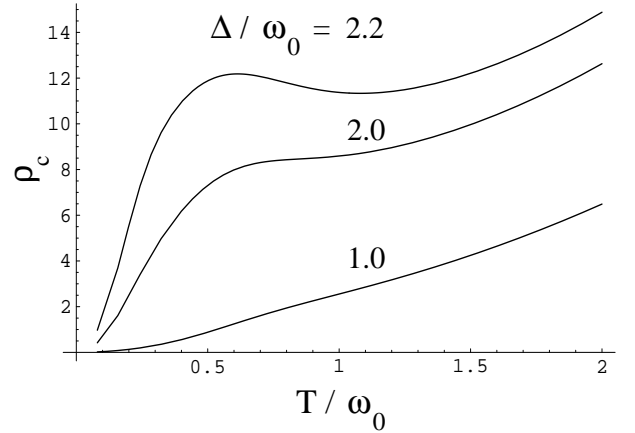


FIG. 3: $B = 0$ c -axis resistivity with in-plane Fermi liquid scattering (Eq. 32) for electrons coupled to c -axis Einstein phonons, $\alpha_{\text{FL}} = 5.0$, $\epsilon_F = 100\omega_0$.

Now we consider the magnetic field dependence. The magnetoresistivity is defined as $\Delta\rho_c = \rho_c(B)/\rho_c(0) - 1$. For later convenience, the effective cyclotron frequency is defined as: $\omega_c = v_F e c B$.

First, at very low T and very large magnetic fields, in Eq. 28 the effective cyclotron frequency can become larger than the scattering rate and so the magnetoresis-

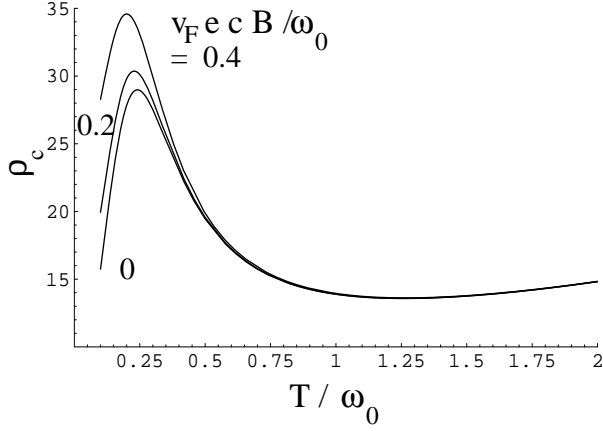


FIG. 4: c -axis resistivity at finite B with in-plane marginal Fermi liquid scattering (Eq. 30), for electrons coupled to c -axis Einstein phonons as a function of T . $\alpha_{\text{MFL}} = 1.0$, $\Delta/\omega_0 = 2.0$.

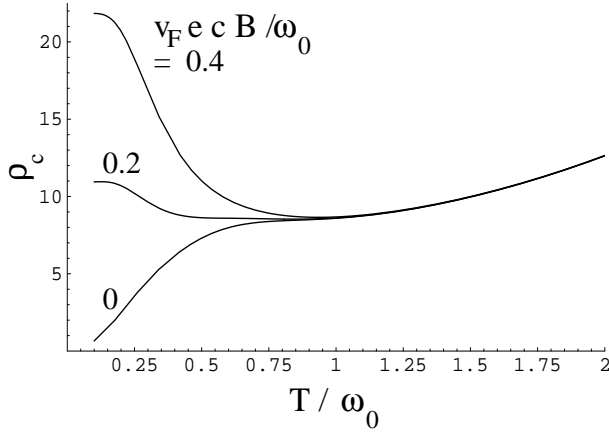


FIG. 5: c -axis resistivity at finite B with in-plane Fermi liquid scattering (Eq. 32), for electrons coupled to c -axis Einstein phonons, as a function of T . $\alpha_{\text{FL}} = 5.0$, $\epsilon_F = 100\omega_0$, $\Delta/\omega_0 = 2.0$.

tance goes as:

$$\Delta\rho_c \propto \omega_c/\Gamma(T), \quad (39)$$

i.e., linearly²⁵ in B . See Fig. 6,7.

At higher T , the scattering rate dominates in both Eqs. 29 and 34. For the $n = 0$ term, $[\omega_c^2 + \Gamma_{\text{tot}}^2]^{-1/2}$ gives a $1 - B^2$ contribution to the conductivity, *i.e.* a $+B^2$ magnetoresistance. For the $n \geq 1$ terms, since $\omega_0 \sim 10^{-2}\epsilon_F$, and $\omega_c \sim 10^{-3}\epsilon_F$ for B up to a few tesla, $\omega_c \ll \omega_0$, we can extract the leading B behaviour of the $n \geq 1$ terms in the conductivity:

$$\begin{aligned} \text{Re} \frac{1}{\sqrt{\omega_c^2 + (\Gamma_{\text{tot}} - i n \omega_0)^2}} &\simeq \frac{\Gamma_{\text{tot}}}{\Gamma_{\text{tot}}^2 + (n \omega_0)^2} \\ &\times \left(1 - \omega_c^2 \frac{\Gamma_{\text{tot}}^2 - 3(n \omega_0)^2}{2[\Gamma_{\text{tot}}^2 + (n \omega_0)^2]^2} + O(\omega_c/\Gamma_{\text{tot}})^4 \right). \end{aligned} \quad (40)$$

While it is possible for the coefficient of the B^2 term in Eq. 40 to change sign, it can be shown that the $n = 0$ term always dominates, leading to a $1 - B^2$ conductivity, or a $+B^2$ magnetoresistance:

$$\Delta\rho_c \propto (\omega_c/\Gamma_{\text{eff}})^2, \quad (41)$$

where the effective scattering rate Γ_{eff} is made up of both the electronic scattering and the phonon frequency, and taking into account only up to $n = 1$ harmonics,

$$\Gamma_{\text{eff}}^2 \approx \frac{\frac{1}{2\Gamma_0} + \frac{4\Gamma_1}{4\Gamma_1^2 + \omega_0^2}}{\frac{1}{16\Gamma_0^3} + \frac{2\Gamma_1(4\Gamma_1^2 - 3\omega_0^2)}{(4\Gamma_1^2 + \omega_0^2)^3}}, \quad (42)$$

where $\Gamma_0 = \Gamma(T, 0)$, and $\Gamma_1 = \Gamma(T, \omega_0)$.

In conclusion, there is positive magnetoresistance at all temperatures and for both Fermi liquid and marginal Fermi liquid in-plane states. In general, if the in-plane scattering $\Gamma(\omega)$ could be made *larger* at $\omega = 0$ relative to the higher harmonics $\omega = n\omega_0$, the contribution of the $n = 0$ part of the phonon function $D(\omega)$ is suppressed, and this can lead to a *negative* magnetoresistance.

Figs. 4,5,6 and 7 illustrate the resistivity as a function of T and B .

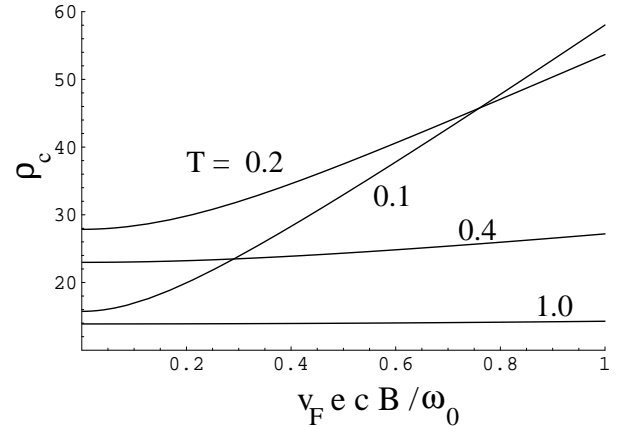


FIG. 6: c -axis resistivity with in-plane marginal Fermi liquid scattering (Eq. 30), for electrons coupled to c -axis Einstein phonons, as a function of B . $\alpha_{\text{MFL}} = 1.0$, $\Delta/\omega_0 = 2.0$. T is measured in units of ω_0 .

B. General phonon dispersion

Having considered an Einstein mode, we now treat a more general dispersing phonon mode. The function $D(\omega, T)$ will be seen to be strongly peaked near $\omega \sim 0$, compared to the in-plane Fermi energy scale ϵ_F . Furthermore, we are in the regime $T/\epsilon_F \ll 1$. Thus, $[f(\nu) - f(\nu + \omega)]/\omega \simeq -\partial f/\partial \nu \simeq \delta(\nu)$. The last approximation is valid for the same reason as in the Einstein

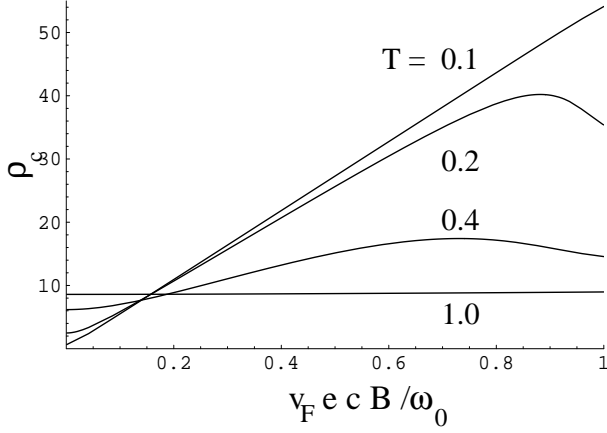


FIG. 7: c -axis resistivity with in-plane Fermi liquid scattering (Eq. 32), for electrons coupled to c -axis Einstein phonons, as a function of B . $\alpha_{\text{FL}} = 5.0$, $\epsilon_F = 100\omega_0$, $\Delta/\omega_0 = 2.0$. T is measured in units of ω_0 .

phonon case. Hence, with these approximations and inserting the gaussian form of the phonon function of Eq. 20 into Eq. 25 leads to

$$\sigma_c(T, B) = \frac{e^2 N_0 N_c t_c^2}{\pi T} e^{-C(T)} \int \frac{d\nu}{\sqrt{\pi \gamma^2(T)}} \frac{\nu}{\sinh \frac{\nu}{2T}} \times \text{Re} \frac{\exp - \frac{\nu^2}{4\gamma^2(T)}}{[(v_F e c B)^2 - (\nu + i\Gamma_{\text{tot}}(T, \nu))^2]^{1/2}}$$

$$C(T) = \sum_q F_q \frac{2 \sinh^2(\frac{\omega_q}{4T})}{\sinh \frac{\omega_q}{2T}} \quad (43)$$

where $F_q = \left| \frac{M_q}{\omega_q} \right|^2 2(1 - \cos q)$ and $\gamma^2(T) = \sum_q F_q |\omega_q|^2 / 2 \sinh(\omega_q/2T)$.

The various parameters have the following limiting values:

$$\gamma^2(T) \rightarrow \begin{cases} 2T\bar{\Delta} & : T \gg \omega_q, \\ \gamma_0^2(T) & : T \ll \omega_q, \end{cases}$$

$$\exp -C(T) \rightarrow \begin{cases} e^{-\bar{\Delta}/T} & : T \gg \omega_q, \\ e^{-\sum_q F_q} & : T \ll \omega_q. \end{cases} \quad (44)$$

$\bar{\Delta} = \sum_q F_q \omega_q / 2$ involves the electron-phonon coupling, together with the phonon dispersion. It characterises the strength of the electron-phonon interaction, and is directly analogous to the parameter Δ for the Einstein phonon case. $\gamma_0^2(T) = \sum_q F_q |\omega_q|^2 \exp -\omega_q/2T$. (Note that the expressions $T \gg \omega_q$ and $T \ll \omega_q$ refer to some typical energy of the phonon dispersion, *e.g.* the Debye frequency.)

In the low temperature limit $T \ll \omega_q$, the phonon spectral function provides a gaussian in frequency with a width $\gamma_0(T)$ which is exponentially narrow in T . Thus in the integral over frequency ($\int d\nu$), only $\nu \approx 0$ contributes. Furthermore, since $T \gg \gamma_0(T)$, the scattering

rate $\Gamma(T, \nu)$ can be taken at zero frequency, for both a Fermi liquid and a marginal Fermi liquid. Then the integral in Eq. 43 can be done immediately, leading to the low T asymptotic form:

$$\sigma_c(T \ll \omega_q, B) = \frac{2e^2 N_0 N_c t_c^2}{\pi \sqrt{(v_F e c B)^2 + 4\Gamma(T, 0)^2}} e^{-\sum_q F_q}. \quad (45)$$

This gives rise then to a low temperature metallic resistivity that tracks the in-plane scattering $\Gamma(T, 0)$, and a positive magnetoresistance with a leading B^2 -dependence, much as in the Einstein phonon case. Note that the hopping matrix element t_c is effectively reduced by the phonon-induced prefactor $\exp -\sum_q F_q/2$, similar to the Einstein phonon case.

In the high temperature limit $T \gg \omega_q$, when $\bar{\Delta} \ll T$, the width of the gaussian $\gamma^2 \sim 2T\bar{\Delta} \ll T^2$, hence again only small frequency $\nu \sim 0$ is needed in the integral in Eq. 43, leading to:

$$\sigma_c(T \gg \omega_q, B) = \frac{2e^2 N_0 N_c t_c^2}{\pi \sqrt{(v_F e c B)^2 + 4\Gamma(T, 0)^2}} e^{-\bar{\Delta}/T}. \quad (46)$$

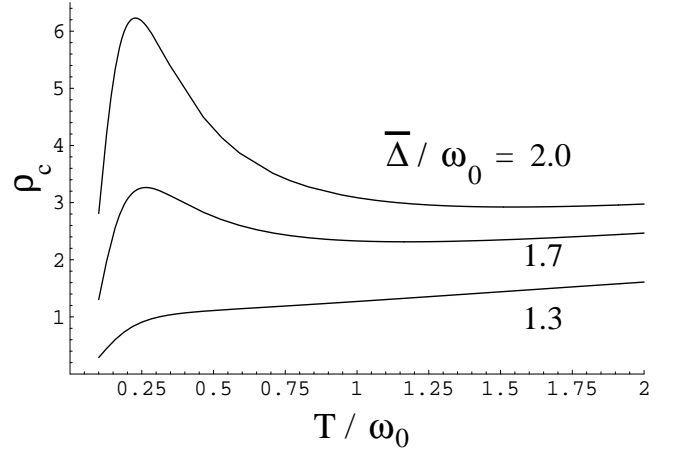


FIG. 8: $B=0$ c -axis resistivity with in-plane marginal Fermi liquid scattering, for the phonon dispersion $\omega_q = \omega_0[1 - 0.4 \cos(q)]$, $\alpha_{\text{MFL}} = 1.0$.

Just as in the Einstein phonon case, there can be a broad maximum structure when $T \sim \omega_q$: it can be shown that in this regime, the phonon contribution $e^{-C(T)}/\gamma(T)$ provides a semi-conducting-like upturn in conductivity, which competes with the in-plane scattering $\Gamma(T, 0)$ that eventually dominates as $T \gg \omega_q$. This is to some extent captured in Eq. 46 above. More precise T -dependence will require an explicit form for the optical phonon dispersion ω_q . For illustration, let $\omega_q = \omega_0[1 - 0.4 \cos(q)]$, and set the electron-phonon coupling M_q to be q -independent. Eq. 43 is then evaluated numerically and plotted: Fig. 8 is for a marginal Fermi liquid form for the in-plane scattering, while Fig. 9 shows the Fermi liquid case. ρ_c is measured in units of

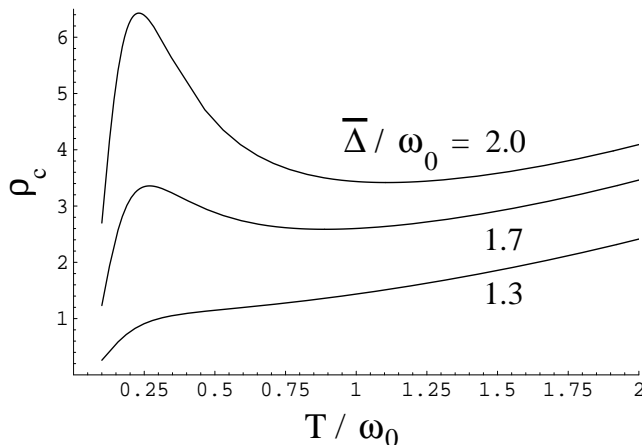


FIG. 9: $B=0$ c -axis resistivity with in-plane Fermi liquid scattering, for the phonon dispersion $\omega_q = \omega_0[1 - 0.4 \cos(q)]$, $\alpha_{\text{FL}} = 5.0$, $\epsilon_F = 100\omega_0$.

$\pi/e^2 N_0 N_c t_c^2$. Qualitatively, these plots are similar to the Einstein phonon ones.

As for the Einstein phonon case, there is only positive magnetoresistance for the more general phonon dispersion, at all temperatures.

V. DISCUSSION

A. Summary of results

In this paper we have studied $2d$ planes of electrons characterised by a Fermi liquid or a marginal Fermi liquid scattering rate (that has little momentum dependence), coupled by a small inter-plane single-particle hopping in the third dimension, in the presence of a strong interaction between electronic density and a bosonic mode in the inter-plane direction. The electron-boson coupling is treated exactly via a canonical transformation, and we treat the inter-plane hopping to lowest order (t_c^2) to calculate conductivity and magnetoconductivity. For concreteness, we have considered the bosonic mode to be a phonon, and have treated two types of phonons: Einstein phonons and a more general dispersing phonon mode. The overall behavior appears to be quite similar for the Einstein mode when compared to the more general phonon dispersion, and we shall discuss them together, pointing out the differences where they arise.

We find that at temperatures low compared to the typical phonon energy, the c -axis resistivity ρ_c is metallic, displaying the same temperature dependence as that of the underlying in-plane scattering rate $\Gamma(T)$: $\rho_c \sim \Gamma(T)$. The magnitude is however strongly reduced, corresponding to a much smaller effective c -axis bandwidth, directly analogous to the bandwidth renormalisation in the Holstein small polaron problem^{10,23}.

At temperatures much much larger than the typical phonon energy, (a regime that is probably academic,)

$\rho_c(T)$ again reflects the T -dependence of the in-plane scattering rate, but in the Einstein phonon case, there is an extra multiplicative factor of $T^{1/2}$ contributed by the phonons, while for the general phonon case, the T -dependence is exactly as in $\Gamma(T)$. Note that it is because of this in-plane factor of $\Gamma(T, \omega)$, that the high temperature state is metallic like (*i.e.* $d\rho_c/dT > 0$), in contrast to the standard Holstein small polaron model.

In the experimentally interesting regime where T is of the same magnitude as the phonon energy (a few hundred Kelvins), we find the possibility in ρ_c of a broad maximum structure that connects the low and high temperature metallic states. For the Einstein phonons, we have shown that this broad maximum, *i.e.* a “non-metallic” T -dependence, occurs *only* when there is strong electron-phonon coupling (Eq. 35). We have also estimated the position and width of the maximum in the temperature axis. For the general phonon dispersion case, we expect, and see numerically, qualitatively similar behavior. Note that the physics is richer here than in the Holstein small polaron problem, due to the extra degree of freedom of the in-plane scattering rate.

As expected, we have found only positive magnetoresistance in our model, since we only consider the effect of the magnetic field pointing in the plane on the orbital motion of the electrons. This goes as $\Delta\rho_c \propto (\omega_c/\Gamma_{\text{eff}})^2$ (Eq. 41), except for the regime when the magnetic field is very large and the temperature is very low, in which case²⁵ $\Delta\rho_c \propto \omega_c/\Gamma(T)$ (Eq. 39). This is so for both the Einstein phonons and the more general phonon dispersion, and for both the marginal Fermi liquid or Fermi liquid scattering rates.

In this work we have tacitly assumed that computing σ_c as an expansion in t_c is valid and that we can fully characterize the in-plane physics by its single particle properties. For non-Fermi liquid states in the plane this may not be the case (a Luttinger liquid in 1D is a notable example²⁶). Under such circumstances our results would presumably breakdown below a temperature scale which would depend on the details of the in-plane physics.

Our model consists of phonons that have no structure in the in-plane direction, and a more realistic model should have a fully three dimensional dispersion. In this respect, a question immediately arises: if the metallic to non-metallic transition in the c direction requires a strong electron-phonon coupling, might not this strong coupling also show up in the in-plane physics? This is presumably a question of scales: the characteristic phonon energy is expected to be larger than the c -axis hopping matrix element t_c , but the phonon energy is still much smaller than the in-plane Fermi energy, because of the highly anisotropic nature of the materials considered here. Hence, one expects the strong electron-phonon coupling to have a much more dramatic effect in the c -direction, than in the in-plane direction.

B. Application to the ruthenate systems

There exist optical phonons with the appropriate symmetry for c -axis transport¹⁶ in Sr_2RuO_4 , and experimentally the broad maximum in the c -axis resistivity has been linked to a structural phase transition¹⁵ in $\text{Ca}_{1.7}\text{Sr}_{0.3}\text{RuO}_4$ at around the broad maximum temperature. Thus one should consider the possibility of electron-phonon interaction affecting the c -axis transport.

In particular, both the Sr_2RuO_4 and $\text{Ca}_{1.7}\text{Sr}_{0.3}\text{RuO}_4$ systems exhibit^{14,15} qualitatively this broad maximum structure found in our simple model, in the c -axis resistivity near to their characteristic (c -axis) phonon energy. In Sr_2RuO_4 there is even the hint of an upturn in resistivity at high temperatures²⁷, and the result plotted in Fig. 2 bears some resemblance to the data of Tyler *et.al.*¹⁴ (their Fig. 3). Also, the broad maximum temperature of $\sim 130\text{K}$ in Sr_2RuO_4 is indeed smaller than the characteristic phonon energy (around 500 to 800 K,¹⁶), consistent with our estimated bound $T_{\text{max}} < 3\omega_0$. Using the value of 500K for ω_0 , we estimate that the electron-phonon coupling parameter Δ is about two times of ω_0 .

However, the negative magnetoresistance seen around the same temperature regime as the broad maximum cannot at present be explained within this phonon-assisted hopping picture. In our simple model here, to obtain negative magnetoresistance robustly, one needs either a phonon function $D(\omega)$ that peaks at a *finite* frequency, and/or an in-plane spectral weight where the scattering rate is smallest at a *finite* frequency. Either of these possibilities suppress the $\omega = 0$ contribution to σ_c (see Eq. 25.) The Kondo effect can give rise to the second possibility, while it is unclear what kind of phonons can lead to the first possibility.

Other factors that we have neglected that could influence the magnetoresistance include the details of the Fermi surface. We have used a flat band with a circular Fermi surface, while experimentally, the β band (which has the largest c -axis dispersion¹²) is nearly a square Fermi surface and moreover, the c -axis electronic dispersion has dependence on the direction in the in-plane momentum space. Also, the RuO_2 planes are staggered from one plane to another, so that an electron hopping from one plane to another does not stay at the same in-plane coordinate \vec{x} as we have assumed in Eq. 5. These facts may lead to a more singular momentum-integrated spectral weight, compared to the form in Eq. 24 used here. But if the spectral weight is now concentrated into a narrower range of momenta, the \vec{B} -induced relative shift in the momenta between the planes would lead to a more positive magnetoresistance.

Alternatively, there may be additional hopping channels that contribute to the negative magnetoresistance, for example, hopping via some intermediate localized state¹⁹.

Next, we discuss spin effects, which have been ignored so far. At least in the low temperature Fermi liquid regime ($T < 25\text{K}$), there are various types of spin fluc-

tuations in Sr_2RuO_4 (both antiferromagnetic²⁸ and q -independent²⁹). In-plane spin fluctuations enhance the in-plane electronic scattering rate. If the applied magnetic field freezes these fluctuations, then one can get a negative magnetoresistance, with the magnetic field pointing in any direction. However, this negative magnetoresistance will be seen in both ρ_c and ρ_{ab} . In Sr_2RuO_4 , c -axis magnetoresistance goes negative above T_{max} for magnetic fields pointing in-plane or in the c -direction, but the in-plane magnetoresistance remains positive¹⁹. Thus one can rule out suppression of in-plane scattering due to magnetic field freezing out spin fluctuations. And if there were spin-fluctuation mediated c -axis hopping, magnetic field may again suppress this, leading to a positive magnetoresistance.

After this work was completed, we learnt that the in-plane spectral weight at temperatures near and above the resistivity maximum temperature may be anomalous³⁰, in contrast to the spectral weight observed in the low temperature Fermi liquid state. In the Introduction, we have pointed to the possibility that anomalous in-plane physics can lead to incoherent c -axis transport, and these recent results suggest that for Sr_2RuO_4 , this needs to be taken into account. However, because of the linkage of the structural phase transition and the resistivity maximum, the strong electron-phonon coupling model is still relevant to the anomalous c -axis transport in $\text{Ca}_{1.7}\text{Sr}_{0.3}\text{RuO}_4$.

C. Boson-electron coupling

Any strong boson-electron coupling can in general be tackled by the present technique. The analysis presented is for the specific case of a neutral, gapped, bosonic mode, as in a phonon. Instead of phonons, there could be magnons or paramagnons describing the effects of spin fluctuations. In addition to the cuprates, other members of the family of strontium/calcium ruthenate exhibit some types of spin fluctuations and work is in progress to check their importance in the c -axis transport. For magnetoresistance the calculation however needs to be modified. In this paper, the effect of magnetic field is purely on the orbital motion of in-plane electrons because there is no direct coupling between the magnetic field and the phonons, which is not the case for (para)magnons.

D. Conclusion

We have demonstrated that a strong coupling between electrons and a bosonic mode in the (weakest) c -direction in a highly anisotropic metal can lead to a broad maximum (metallic to non-metallic crossover) in the c -axis resistivity. For the case where the boson is a phonon, we have discussed the potential application of the model to Sr_2RuO_4 and its relative $\text{Ca}_{1.7}\text{Sr}_{0.3}\text{RuO}_4$. Despite certain simplifying features of the model, the qualitative

properties of this crossover in these layered ruthenates are captured succinctly. Work in progress will address the issue of the anomalous c -axis magnetoresistance in Sr_2RuO_4 within this framework, and also the effect of the anomalous in-plane spectral weight on c -axis transport in Sr_2RuO_4 . Also we are currently studying other signatures in transport properties of this strong electron-boson coupling, for example, in thermal conductivity.

After completion of this work, we became aware of some related work by Lundin and McKenzie concerning a related small polaron model for intra- and interlayer

transport [cond-mat/0211yyy]. We thank them for sending us a copy of their preprint prior to submission.

Acknowledgement The authors are pleased to acknowledge useful and stimulating discussions with Profs. M. Braden, V. Kravtsov, Y. Maeno, A. Mackenzie, P. Johnson, and Yu Lu.

-
- ¹ Current address: School of Physics and Astronomy, Birmingham University, Edgbaston, Birmingham B15 2TT, U.K.
 - ² For some recent reviews of many of the theoretical concepts, see for example, C.M. Varma, Z. Nussinov, W. v.Saarloos, cond-mat/0103393 (2001), and E.W. Carlson *et.al.*, cond-mat/0206217 (2002).
 - ³ A.J. Leggett, *Braz. J. Phys.* **22**, 129 (1992).
 - ⁴ S.L. Cooper and K.E. Gray, p.61, in “Physical Properties of High Temperature Superconductors” vol. IV, ed. D.M. Ginsberg, World Scientific, Singapore (1994).
 - ⁵ For a review, see P.W. Anderson, “The Theory of Superconductivity in the High T_c cuprates”, Princeton University Press, Princeton (1997).
 - ⁶ L.B. Ioffe and A.J. Millis, *Science*, **285**, 1241 (1999).
 - ⁷ P.B. Littlewood and C.M. Varma, *Phys. Rev. B* **45**, 12636 (1992).
 - ⁸ A.G. Rojo and K. Levin, *Phys. Rev. B* **48**, 16861 (1993), see also, N. Kumar, T.P. Pareek, A.M. Jayannavar, *Phys. Rev. B* **57**, 13399 (1998).
 - ⁹ M. Turlakov and A.J. Leggett, *Phys. Rev. B* **63**, 64518 (2001).
 - ¹⁰ T. Holstein, *Ann. Physics* **8**, 343 (1959).
 - ¹¹ The concept of a small polaron is here generalized slightly to mean that the electron is dressed by a local cloud of neutral bosons, not necessarily of phononic origin.
 - ¹² The best demonstration of the Fermi liquid state is from de Haas van Alphen measurements, A.P. Mackenzie *et.al.*, *Phys. Rev. Lett.*, **76**, 3786 (1996), C. Bergemann *et.al.*, *Phys. Rev. Lett.*, **84**, 2662 (2000). For Fermi liquid-like thermodynamics, see Y. Maeno *et.al.*, *J. Phys. Soc. Japan*, **66**, 1405 (1997).
 - ¹³ T. Katsufuji, M. Kasai, Y. Tokura, *Phys. Rev. Lett.*, **76**, 126 (1996).
 - ¹⁴ A.W. Tyler *et.al.*, *Phys. Rev. B* **58**, 10107 (1998).
 - ¹⁵ R. Jin *et.al.*, cond-mat/0112405 (2001).
 - ¹⁶ For lanthanum cuprates, where the parent compound is isostructural to Sr_2RuO_4 , there has been a lot of experimental and theoretical work on phonons. Here, the mode that can couple to c -axis transport¹⁷ is the axial O_z mode, near the Z point in the Brillouin Zone (ie, $(0,0,2\pi/c)$). This mode has the strongest electron-phonon coupling in the whole zone and behaves like an Einstein phonon.¹⁸ A similar mode has been seen in inelastic neutron scattering in Sr_2RuO_4 , M. Braden *et.al.*, unpublished and personal communication.
 - ¹⁷ For a review of inelastic neutron scattering experiments de-termination of the phonon spectrum, see L. Pintschovius and W. Reichardt, p.295, in “Physical Properties of High Temperature Superconductors” Vol. IV, ed. D. M. Ginsberg, World Scientific, Singapore (1994).
 - ¹⁸ C. Falter, M. Klenner, and W. Ludwig, *Phys. Rev. B* **47**, 5390 (1993), H. Krakauer, W.E. Pickett, and R.E. Cohen, *Phys. Rev. B* **47**, 1002 (1993).
 - ¹⁹ N.E. Hussey *et.al.*, *Phys. Rev. B* **57**, 5505 (1998).
 - ²⁰ See for example: LSCO: T. Kumura *et.al.*, *Phys. Rev. B* **53**, 8733 (1996), N.E. Hussey *et.al.*, *Phys. Rev. B* **58**, 611 (1998). BSCCO and YBCO: Y.F. Yan *et.al.*, *Phys. Rev. B* **52**, 751 (1995). Bi-2201: S.I. Vedenev, A.G.M. Jansen and P. Wyder, *Phys. Rev. B* **62**, 5597 (2000). Bi-2212: G. Heine *et.al.*, *Phys. Rev. B* **59**, 11179 (1999).
 - ²¹ H. Frohlich, *Adv. Phys.* **3**, 325 (1954). For a review, see eg. Mahan²³.
 - ²² I.G. Lang and Yu.A. Firsov, *Sov. Phys. JETP* **16**, 1301 (1963).
 - ²³ G.D. Mahan, “Many-Particle Physics” 2nd Ed., Plenum (1990).
 - ²⁴ Note that when ω_0 is a phonon scale, it is unlikely that the scattering rate in real materials can retain the Fermi liquid form (Eq. 32) for energy or temperature approaching ω_0 , because in-plane phonons will significantly modify the form of this scattering rate. However, if ω_0 is an anomalously small scale (*e.g.* some small magnetic scale), then the in-plane scattering rate may still retain the Fermi liquid form above ω_0 , and we can take Fig. 3 at face value. In Sr_2RuO_4 , the in-plane resistivity starts to deviate from the Fermi liquid form well before T_{max} .¹⁴ the marginal Fermi liquid form is more appropriate for most temperatures.
 - ²⁵ A.J. Schofield and J.R. Cooper, *Phys. Rev. B* **62**, 10779 (2000).
 - ²⁶ C. Bourbonnais and L.G. Caron, *Int. J. Mod. Phys. B* **5**, 1033 (1991).
 - ²⁷ However, we should point out that these resistivity measurements are carried out at constant pressure, while our calculation is for constant volume. This upturn at high temperatures may disappear once the thermal expansion is taken into account.
 - ²⁸ Y. Sidis *et.al.*, *Phys. Rev. Lett.*, **83**, 3320 (1999), F. Servant *et.al.*, *Phys. Rev. B* **65**, 184511 (2002).
 - ²⁹ K. Ishida *et.al.*, *Phys. Rev. B* **64**, 100501 (2001), T. Imai *et.al.*, *Phys. Rev. Lett.*, **81**, 3006 (1998), H. Mukuda *et.al.*, *J. Phys. Soc. Japan*, **67**, 3945 (1998).
 - ³⁰ P. Johnson, private communications.